Front. Phys., 2013, 8(5): 509–515
DOI 10.1007/s11467-013-0386-9

RESEARCH ARTICLE

Modifying optical properties of ZnO nanowires via strain-gradient

Xue-Wen Fu[1,§], **Qiang Fu**[1,§], **Liang-Zhi Kou**[2], **Xin-Li Zhu**[1], **Rui Zhu**[1], **Jun Xu**[1], **Zhi-Min Liao**[1], **Qing Zhao**[1], **Wan-Lin Guo**[2,*], **Da-Peng Yu**[1,†]

[1] *State Key Laboratory for Mesoscopic Physics, and Electron Microscopy Laboratory, Department of Physics, Peking University, Beijing 100871, China*

[2] *State Key Laboratory for Mechanics and Control of Mechanical Structures, and MOE Key Laboratory of Intelligent Nano Materials and Devices, Institute of Nano Science, Nanjing University of Aeronautics and Astronautics, Nanjing 210016, China*

*Corresponding authors. E-mail: * wlguo@nuaa.edu.cn, † yudp@pku.edu.cn*

Received August 8, 2013; accepted August 29, 2013

We conduct systematical cathodoluminescence study on red-shift of near-band-edge emission energy in elastic bent ZnO nanowires with diameters within the exciton diffusion length (∼ 200 nm) in liquid nitrogen temperature (81 K). By charactering the emission spectra of the nanowires with different local curvatures, we find a linear relationship between strain-gradient and the red-shift of near-band-edge emission photon energy, an elastic strain-gradient effect in semiconductor similar to the famous flexoelectric effect in liquid crystals. Our results provide a new route to understand the inhomogeneous strain effect on the energy bands and optical properties of semiconductors and should be useful for designing advanced nano-optoelectronic devices.

Keywords strain-gradient, ZnO nanowire, cathodoluminescene, exciton energy, energy bands

PACS numbers 73.20.At, 78.20.hb, 77.65.Ly

Elastic strain engineering has become an important technology in microelectronic industry since the 90 nm chips in 2003 [1, 2]. Entering the nanoscale, many semiconducting crystals become more tough and flexible and strains become more localized and inhomogeneous accompanied by high strain-gradient [3, 4]. The strain-gradient effect has been recognized to play an important role in many functional media [5, 6], such as the "flexoelectricity", a linear response of polarization to strain-gradient found in liquid crystals [7] and crystalline dielectric [8]. However, the role of strain-gradient in semiconductors still remains elusive, although the concerns about inhomogeneous strain effect on band structures of semiconductors have been raised for half century [9, 10]. Nanowires have been attracting great attention for possible applications, especially the ZnO nanowires which are sensitive to deformation and have wide range of potential applications [11]. Such as bending ZnO micro/nanowires have given rise to novel nanogenerators [12] and piezotronic devices [13]. Elastically curved nanowires are ideal platforms for studying the strain-gradient effect as the strain changes linearly across the section [14, 15], leading to a constant strain-gradient on given section, and the strain-gradient is determined by the local bending curvature.

In this paper, we find a linear relationship between the strain-gradient and red-shift of the near-band-edge (NBE) emission energy through systematical spot-scanning cathodoluminescence (CL) studies along bent ZnO nanowires with diameter ranging from 80 to 160 nm at low temperature (∼81 K). The linear relationship is due to the coupling change of electronic energy states in the tensile and compressive parts through exciton diffusion, which is supported by density functional calculations. The linear strain-gradient effect on the NBE emission energy of semiconductors provide a new route to understand the inhomogeneous strain effect on the optical properties of semiconductors, and it could be very useful for designing advanced nano-photonic and electronic devices.

§ These authors contributed equally to this work.

The ZnO nanowires investigated here were synthesized through the simple chemical vapor deposition (CVD) method [16]. All the ZnO nanowires grew along the [0001] zone axis with hexagonal cross-section, which was evident from high resolution TEM characterization, as shown in Figs. 1(a) and (b). After growth, the nanowires were then dispersed in ethanol and transferred to a silicon wafer with predefined marks for identifying and coordinating nanowires of interest. The nanowires were manipulated, using a glass tip under an optical microscope (Olympus, BX51M), to curved configurations. The curved configuration was preserved even after removing the glass tip, which is due to the strong van der Waals interaction between the nanowire and the substrate. The re-straightening of the nanowire in contact to a drop of ethanol supports this supposition and shows the deformation to be elastic [see Figs. 1(c) and (d)]. Considering the small size of the nanowires and interactions preserving the nanowire in a curved configuration are local distributed, it is reasonable to regard the bending deformation as pure bending [14]. To describe the local strain state, we define the direction parallel to the substrate surface as x, and the direction vertical to the substrate surface as y, as illustrated in the inset of Fig. 2(a). The lattice in the curved nanowire is distorted and the strain ε_c in a cross section of the curved nanowires varies linearly from compression to tension along its width direction x across a neutral plane, coinciding with the geometry middle-plane at x =0 of the wires. This leads to a constant strain-gradient $g = \frac{\partial \varepsilon_c}{\partial x}$ through the section. In a section with a local curvature radius ρ, $g = 1/\rho$, and $\varepsilon_c = xg = x/\rho$.

The bent ZnO nanowires were characterized by high spatial (100 nm for ZnO) and spectral resolution (0.5 nm) CL at liquid nitrogen temperature (~81 K). The spectra were acquired by CCD with a scan range from 340 to 410 nm. An optimal setting is chosen (voltage of

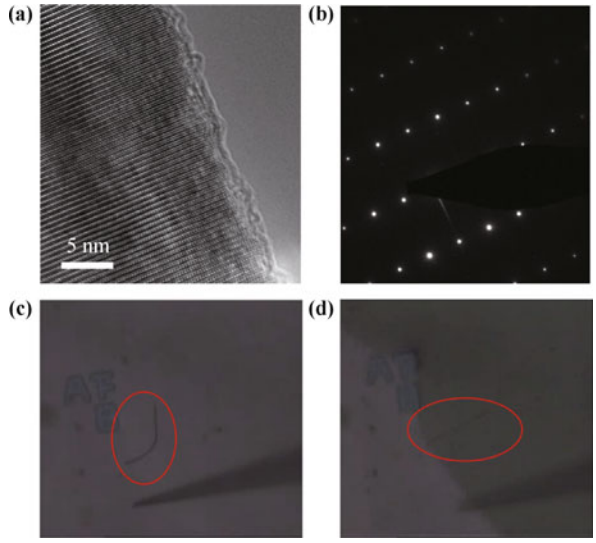

Fig. 1 **(a, b)** High resolution TEM image and diffraction image of a representative ZnO grew along [0001]. **(c)** Photo microscopy image of a bent ZnO nanowire. **(d)** Photo microscopy image of strain released ZnO nanowire. The red eillpse indicates the positon of the nanowire for obvious view.

10 keV and spot size of 4 with the beam current of about 0.353 nA) to achieve the optimum spatial resolution with a high signal-to-noise ratio. Under our experimental settings, the effective region of electron beam in ZnO is ~ 100 nm (with 90% power in this region, supported by Monte Carlo simulation [17]). All measurements were made by point scanning along the axial direction in curved nanowires with the electron beam focused at the center of the nanowires, as indicated by colored circles along the nanowires in Fig. 2(a). Figure 2(b) presents the CL spectra obtained from regions of different curvature radius. When the electron beam was focused on one free end, a peak of NBE emission centered at about 3.355 eV can be observed (a blue shift under low temperature, compared with 3.28 eV at room temperature). Meanwhile, moving to bent positions, the

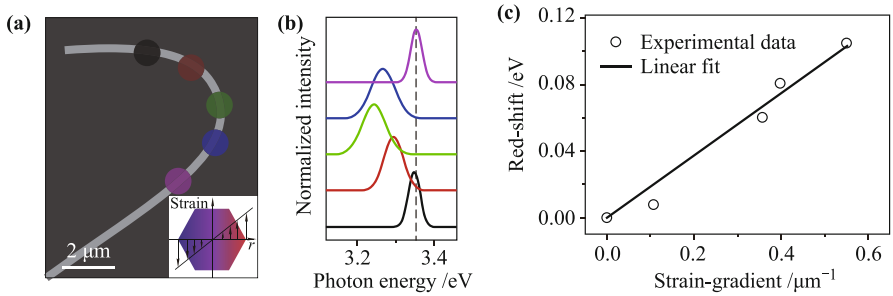

Fig. 2 Linear strain-gradient effect on bent ZnO nanowire: **(a)** SEM image of a bent ZnO nanowire with a diameter of 120 nm. The coloured circles indicate the scanning sites of point-scanning CL spectra. The inset illustrates the strain distribution on the cross section of the bent ZnO nanowire. **(b)** CL spectra obtained from the bent nanowire at sites indicated in (a) and smoothened by Gaussian fitting. Each curve is coloured with the same color as the site indicating circle in (a). The dashed line shows the origin position of the NBE emission peak is 3.355 eV at ~81 K. **(c)** Linear red-shift of the NBE emission peak against the strain-gradient.

NBE emission peak red shifted, revealing a reduction of band gap. The red-shift enhanced with the increase of strain-gradient g, and returned to the original position when the exciting electron beam arrives at the other free end. The maximum red-shift in this sample is up to ~100 meV. Figure 2(c) shows the experimental results of strain-gradient induced red-shift of NBE emission energy. Clearly, the red-shift of NBE emission energy ΔE bears a linear relationship with the strain-gradient g,

$$\Delta E = \hbar c \beta g \tag{1}$$

In the expression, β is the strain-gradient effect coefficient, and $\hbar c = 1.23982\ \text{eV}\cdot\mu\text{m}$ is the product of Planck's constant with the speed of light. This linear relationship is identified in all the ZnO nanowire samples differing in curved shapes, and with varying diameters of 80–160 nm

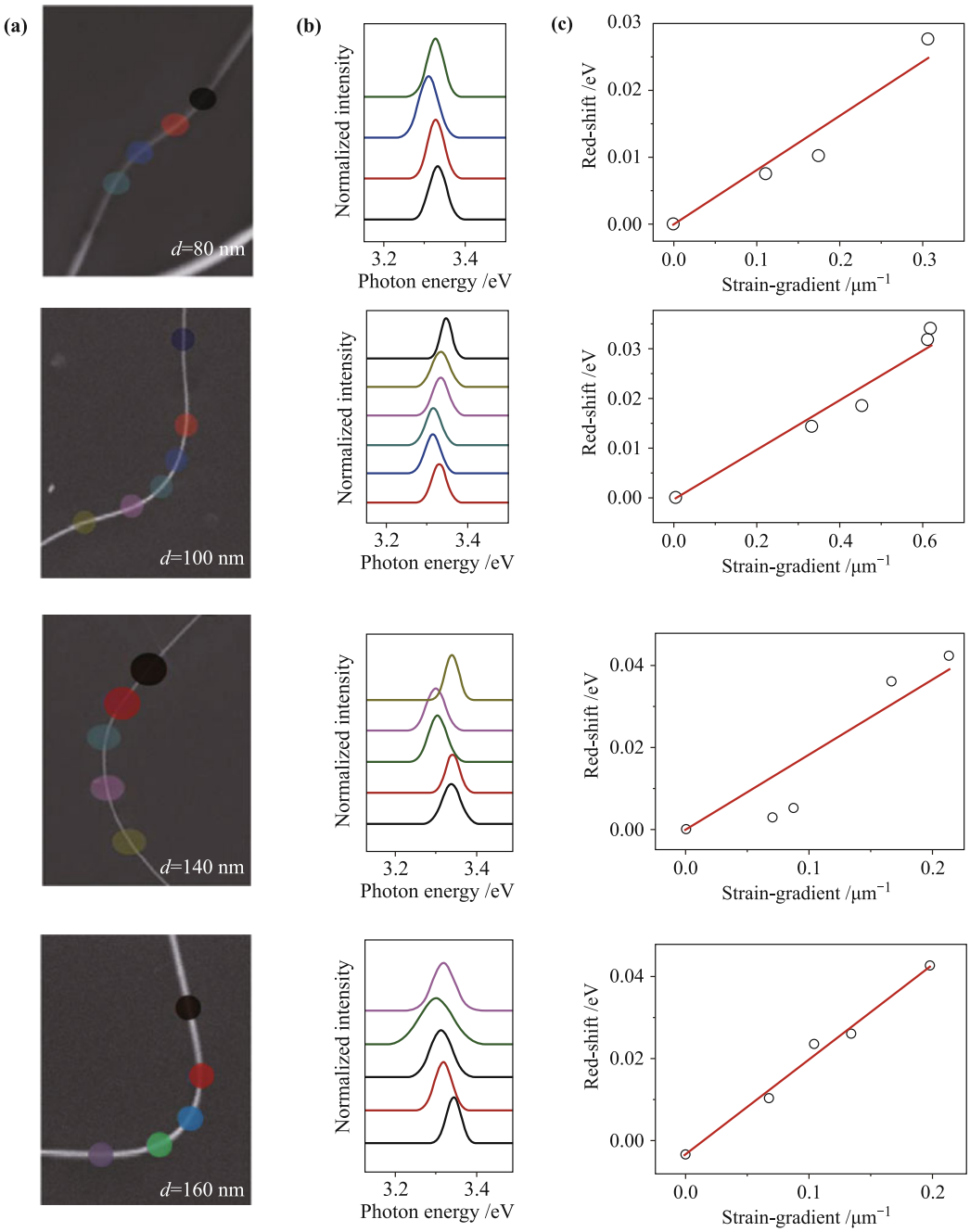

Fig. 3 Linear strain-gradient effect on another four bent ZnO nanowires with different diameters. **(a)** SEM images of the bent ZnO nanowires with a diameter of 80 nm, 100 nm, 140 nm, and 160 nm, respectively. The coloured circles indicate the scanning areas of spot-scanning CL spectra. **(b)** CL spectra obtain from (a) (fitted by Gauss for smoothing). The spectra curves have corresponding colours with the circles in (a). **(c)** The linear relationship between strain-gradient and red-shift of the NBE emission peak.

(results from more than ten samples), the detail results are presented in Fig. 3.

The observed experimental results can be explained as energy states coupling by exciton diffusion in the bent ZnO nanowire. Normally, the red-shift and blue-shift of NBE emission photon energy are caused by tensile and compressive strain, respectively. However, as the diameters of the nanowires approach the exciton diffusion length (for ZnO material it is about 200 nm at 81 K [18, 19]), the energy states of the tensile and compressive regions could be coupled by the exciton diffusion effect.

To have a further understanding of the observed linear strain gradient effect, first-principled calculations were carried out on strained bulk ZnO crystal. The strain was applied to the lattice along the c-axis. Then, calculations are carried out with the linear combination of atomic orbital basis implemented in the SIESTA package [20], using the Perdew–Burke–Ernzerh (PBE) [21] of generalized gradient approximation (GGA) for the exchange correlation energy and norm-conserving pseudopotentials for the core-valence interactions. The double-ζ polarized numerical atomic-orbital basis sets for Zn and O are used. 6×6×4 Monkhorst–Pack k-point grid is used in the energy calculations. An energy cutoff of 500 Ry is sufficient to converge the grid integration of the charge density, and atomic positions are fully relaxed under applied strain using a conjugate gradient method so that the force on each atom is less than 0.02 eV/Å. All these pseudopotentials and parameters adopted here have been successfully used in ZnO nanostructures in our previous work [22, 23], and their validity has been well established.

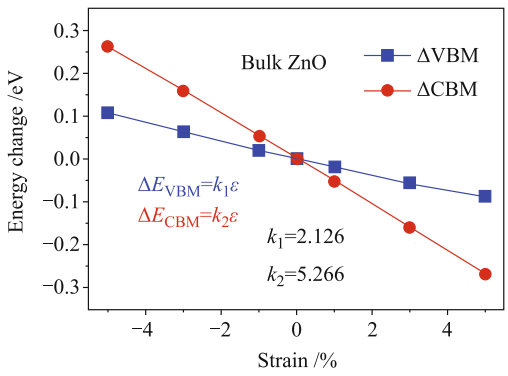

Fig. 4 Calculation result of the energy change of band-edge states as a function of applied strain along the c axis. A prefect linear relationship between energy change of band-edge states and strain is revealed.

Figure 4(a) plots the density functional calculation results of the valance band maximum (VBM) and conduction band minimum (CBM) in bulk ZnO material under c-axis strain; the plus and minus indicates tensile and compressive strain, respectively. Clearly, the variation in VBM and CBM can be described as a linear relationship with strain ε_c,

$$\Delta E_{\mathrm{VBM}} = k_1\varepsilon_c, \quad \Delta E_{\mathrm{CBM}} = k_2\varepsilon_c \tag{2}$$

The states in inner and outer sides are coupled by exciton diffusion effect in bent ZnO nanowires with diameters within the exciton diffusion length, and result in a reduction in the band gap, coinciding with a red-shift in the final NBE emission peak. The photon energy red-shift in the bending region is determined by the variations of VBM and CBM states under bending deformation. The reduced band gap E_g can be calculated as

$$E_g = E_0 - \Delta E_g \tag{3}$$

E_0 in the expression refers to the band gap of strain free ZnO crystal. For a lattice under symmetric pure bending strain, the variation of band gap ΔE_g bears a relationship with strain gradient

$$\begin{aligned}\Delta E_g &= \int \mathrm{d}E_g = \int \frac{\partial E_g}{\partial x}\mathrm{d}x \\ &= \int (|k_1| + |k_2|)\frac{\partial \varepsilon_c}{\partial x}\mathrm{d}x \propto g\end{aligned} \tag{4}$$

Our observed linear relationship between strain-gradient and band-gap energy is similar to the linear response of polarization to strain-gradient (flexoelectric effect) in dielectrics [24]. Here, the linear strain-gradient coefficient β can be obtained by fitting the experimental data. It seems that the linear strain-gradient coefficient β increases with the diameter of nanowire, as shown in Fig. 5(a). Another noteworthy point is that when focusing in the bent region, a broadening of the NBE emission peak can be observed. This is ascribed to the breaking of the strict crystal symmetry by inhomogeneous strain [14]. This breaking of the strict crystal symmetry would split and broaden the narrow bands in the otherwise perfect crystal, resulting in a broadening of the NBE emission peak. The relationship between the peak position and the full width at half-maximum (FWHM) indicates that FWHM increases with the red-shift of exciton energy [see Fig. 5(b)].

To verify our theory analysis, we also conduct density functional calculations on cosine curved ZnO nanowires along [0001] direction. The results shown in Table 1 indicate that the simulated band gap in curved ZnO nanowires is consistent with the predicted value by our formula. Therefore our theory is simple and effective in revealing the underlying influence of strain gradient on the optical properties of semiconductor nanowires.

When the diameter of the nanowire is much larger than the exciton diffusion length, the energy states in the tensile and compressive parts could not be coupled by

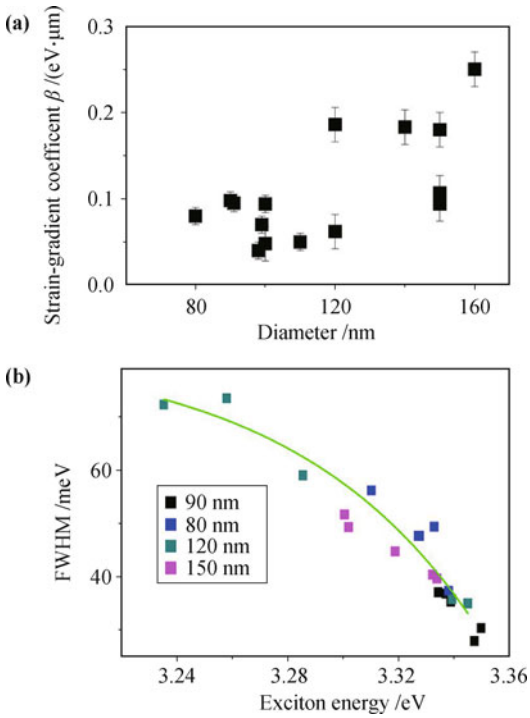

Fig. 5 Size dependence of the strain-gradient effect. **(a)** Experimental results of the dependence of strain-gradient coefficient β upon the diameter of the bent nanowires. **(b)** The relationship of full width at half-maximim (FWHM) with the exciton emission peak position.

Table 1 Density functional calculations (DFT) results of band gap and the predicted value by our formula. The well consistence indicates that our theory is simple and effective.

Diameter /nm	Amplitude of cosine curved lattice /Å	Band gap calculated by curved lattice /eV	Band gap calculated by simplified formula /eV
0.97	1.25	1.08	1.14
1.62	1.25	0.93	0.92

exciton diffusion when the excitation spot moving beyond the strain-neutral-middle-plane. Under this condition, an asymmetric red-shift and blue-shift can be observed along the radial direction [14], as demonstrated in the line-scanning CL measurement results in Fig. 6.

As the exciton Bohr radius of ZnO is about 2.34 nm [25], which is much smaller than the diameter of the nanowires used in this work, quantum confinement effect can be neglected. Another possible concern is that the red-shift of exciton energy might have been induced by electron beam irradiation effects of in situ CL measurements. The dependence of ZnO CL spectra on irradiation duration shown in Ref. [26] indicates that the intensity of the CL spectra decreases with the irradiation duration, but the exciton energy remains stable under irradiation for long duration. The built up of transverse potential field through piezoelectric effects in bent ZnO

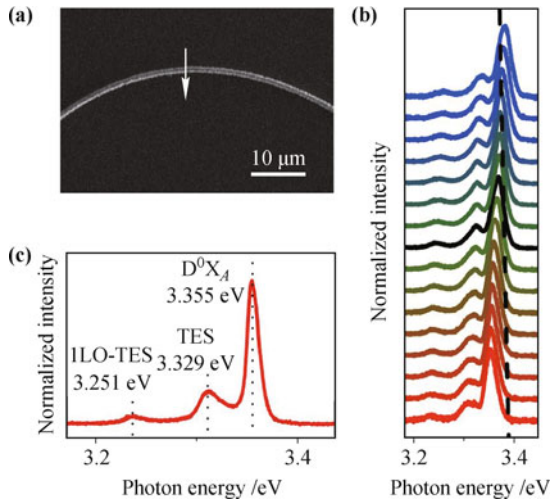

Fig. 6 Line-scanning CL spectra along the radial direction of bent ZnO microwire. **(a)** A bent microwire with a diameter of 1μm. The white arrow marked the cross section where we made the line-scanning. **(b)** The CL spectra obtained from the cross section marked with white arrow in (a). The black coloured curve is the spectra of the strain-neutral middle-plane, and the dotted line marked the origin position of D^0X_A exciton peak (3.355 eV). **(c)** CL spectra of strain-free area. The dotted lines marked the peaks of D^0X_A, TES and 1LO-TES, respectively.

nanowires may also be a possible contributor to the observed red-shift. Nevertheless, such a field is only up to 1.8 mV/nm according to the best existing experimental reports on ZnO wires [27]. Our density functional calculations show that such a field with strength of 20 mV/nm can only lead to a band gap variation of 0.8 meV, and the influence can become significant only when the field strength is over 1 V/nm. Therefore, the piezoelectric effect induced transverse potential field could have some contribution, but it should be a secondary influence factor. The bending strain and its gradient are the dominating effects on the electronic energy bands and the NBE emission energy of bent ZnO nanowires.

The shear strain may also have contribution to the red-shift. In our experiments, different manipulation and resulted curving deformation should induce different shear strain if it exists, but the linear relationship is confirmed in all the investigated samples. This means that measured linear red-shift with strain gradient should be mainly due to bending deformation. Therefore, the effect of shear strain, if it exists, can be secondary or neglectable in the present experiments.

In conclusion, we find a linear strain-gradient effect on the NBE emission photon energy of ZnO nanowires through systematical low temperature CL investigation in bent ZnO nanowires with diameters within the exciton diffusion length. The linear relationship between the red-shift of NBE emission photon energy and the strain gradient can be explained by the coupling energy states

in the tensile and compressive sides of the bent nanowire via exciton diffusion effect. This linear strain-gradient effect on the energy bands and exciton energy of semiconductors shed a new light on energy band theory and optical properties of semiconductors in inhomogeneous strain fields. And it should be important to the development of flexible nano-optoelectronic devices.

Experimental section

ZnO nanowires growth method: Pure zinc phosphate powder (99 %) and graphite mixed in molar ratio 1 were loaded in an alumina boat. A piece of (001) sapphire chip was placed above the zinc phosphate powder as the collecting substrate. The boat was then placed at the center of a quartz tube and inserted into a rapid heating furnace. In the furnace, the tube was purged of contaminants using Argon gas for ten minutes, after which, as the growth carrier gas, argon was maintained at 200 sccm flow. The furnace was heated up to 1050°C in 20 min and held for 1 min before cooling down to room temperature naturally, after which oxygen (2.6 sccm) was introduced as the reactive gas at 1050°C. After growth, the substrate was covered by a layer of wax-like product. All the ZnO nanowires grew along the [0001] zone axis with hexagonal cross-section, which was evident from high resolution TEM images.

CL measurement method: To obtain the optimum spatial resolution with best signal-to-noise ratio, an electron beam was accelerated at 10 kV voltage (spot size 4 with the beam current of about 0.353 nA), which results in the effective interaction of electron beam in ZnO ranging about 100 nm (with 90% power in this region, as supported by Monte Carlo simulation [17]). The spot scanning CL spectra were carefully collected with electron beam focused at the neutral plane along the bent ZnO nanowires by CL spectroscopy (Gatan monocle 3+) at liquid nitrogen temperature (~81 K). The CL spectra were recorded by CCD (Charge Coupled Device) with a scanning range of 300 to 450 nm with spectral resolution of about 0.5 nm.

Acknowledgements This study was supported by the National Natural Science Foundation of China (NSFC), the State Key Research Projects for Fundamental Science of Ministry of Science and Technology (Grant Nos. 2007CB936200 and 2009CB623703), and the Natural Science Foundation of Jiangsu Province of China.

References and notes

1. V. M. Pereira and A. H. Castro Neto, Strain engineering of graphene's electronic structure, *Phys. Rev. Lett.*, 2009, 103(4): 046801
2. A. Maiti, Carbon nanotubes: Bandgap engineering with strain, *Nat. Mater.*, 2003, 2(7): 440
3. C. Q. Chen, Y. Shi, Y. S. Zhang, J. Zhu, and Y. J. Yan, Size dependence of Young's modulus in ZnO nanowires, *Phys. Rev. Lett.*, 2006, 96(7): 075505
4. S. Xu, Y. Qin, C. Xu, Y. Wei, R. Yang, and Z. L. Wang, Self-powered nanowire devices, *Nat. Nanotechnol.*, 2010, 5(5): 366
5. K. Kash, B. P. Van der Gaag, D. D. Mahoney, A. S. Gozdz, L. T. Florez, J. P. Harbison, and M. Sturge, Observation of quantum confinement by strain gradients, *Phys. Rev. Lett.*, 1991, 67(10): 1326
6. B. A. Bernevig and S.-C. Zhang, Quantum spin Hall effect, *Phys. Rev. Lett.*, 2006, 96(10): 106802
7. J. Harden, B. Mbarga, N. Éber, K. Fodor-Csorba, S. Sprunt, J. T. Gleeson, and A. Jákli, Giant flexoelectricity of bent-core nematic liquid crystals, *Phys. Rev. Lett.*, 2006, 97(15): 157802
8. A. K. Tagantsev, Piezoelectricity and flexoelectricity in crystalline dielectrics, *Phys. Rev. B*, 1986, 34(8): 5883
9. M. Leong, B. Doris, J. Kedzierski, K. Rim, and M. Yang, Silicon device scaling to the sub-10-nm regime, *Science*, 2004, 306(5704): 2057
10. J. Cao, E. Ertekin, V. Srinivasan, W. Fan, S. Huang, H. Zheng, J. W. L. Yim, D. R. Khanal, D. F. Ogletree, J. C. Grossman, and J. Wu, Strain engineering and one-dimensional organization of metal–insulator domains in single-crystal vanadium dioxide beams, *Nature Nanotech.*, 2009, 4(11): 732
11. Ü. Özgür, Ya. I. Alivov, C. Liu, A. Teke, M. A. Reshchikov, S. Dogan, V. Avrutin, S. J. Cho, and H. Morkoç, A comprehensive review of ZnO materials and devices, *J. Appl. Phys.*, 2005, 98(4): 041301
12. Y. Qin, X. Wang, and Z. L. Wang, Microfibre–nanowire hybrid structure for energy scavenging, *Nature*, 2008, 451(7180): 809
13. Z. L. Wang and J. Song, Piezoelectric nanogenerators based on zinc oxide nanowire arrays, *Science*, 2006, 312(5771): 242
14. X. B. Han, L. Z. Kou, X. L. Lang, H. B. Xia, N. Wang, R. Qin, J. Lu, J. Xu, Z. M. Liao, X. Z. Zhang, X. D. Shan, X. F. Song, J. Y. Gao, W. L. Guo, and D. P. Yu, Electronic and mechanical coupling in bent ZnO nanowires, *Adv. Mater.*, 2009, 21(48): 4937
15. X. B. Han, L. Z. Kou, X. L. Lang, H. B. Xia, N. Wang, R. Qin, J. Lu, J. Xu, Z. M. Liao, X. Z. Zhang, X. D. Shan, X. F. Song, J. Y. Gao, W. L. Guo, and D. P. Yu, Strain-gradient effect on energy bands in bent ZnO microwires, *Adv. Mater.*, 2012, 24(34): 4707
16. J. Y. Gao, X. Z. Zhang, Y. H. Sun, Q. Zhao, and D. P. Yu, Compensation mechanism in N-doped ZnO nanowires, *Nanotechnology*, 2010, 21(24): 245703

17. J. Xu, L. Chen, L. S. Yu, H. Liang, B. S. Zhang, and K. M. Lau, Cathodoluminescence study of InGaN/GaN quantum-well LED structures grown on a Si substrate, *J. Electron. Mater.*, 2007, 36(9): 1144
18. J. Yoo, G. C. Yi, and L. S. Dang, Probing exciton diffusion in semiconductors using semiconductor-nanorod quantum structures, *Small*, 2008, 4(4): 467
19. R. L. Weiher and W. C. Tait, Mixed-mode excitons in the photoluminescence of zinc oxide-reabsorption and exciton diffusion, *Phys. Rev. B*, 1972, 5(2): 623
20. J. M. Soler, E. Artacho, J. D. Gale, A. García, J. Junquera, P. Ordejón, and D. And Sánchez-Portal, The SIESTA method for *ab initio* order-N materials simulation, *J. Phys.: Condens. Matter*, 2002, 14(11): 2745
21. J. P. Perdew, K. Burke, and M. Ernzerhof, Generalized gradient approximation made simple, *Phys. Rev. Lett.*, 1996, 77(18): 3865
22. C. Li, W. Guo, Y. Kong, and H. Gao, First-principles study on ZnO nanoclusters with hexagonal prism structures, *Appl. Phys. Lett.*, 2007, 90(22): 223102
23. L. Kou, C. Li, Z. Zhang, and W. Guo, Electric-field- and hydrogen-passivation-induced band modulations in armchair ZnO nanoribbons, *J. Phys. Chem. C*, 2010, 114(2): 1326
24. R. Resta, Towards a bulk theory of flexoelectricity, *Phys. Rev. Lett.*, 2010, 105(12): 127601
25. Y. Gu, I. L. Kuskovsky, M. Yin, S. O'Brien, and G. F. Neumark, Quantum confinement in ZnO nanorods, *Appl. Phys. Lett.*, 2004, 85(17): 3833
26. S. Achour, A. Harabi, and N. Tabet, Cathodoluminescence dependence upon irradiation time, *Mater. Sci. Eng. B*, 1996, 42(1–3): 289
27. M. P. Lu, J. Song, M. Y. Lu, M. T. Chen, Y. Gao, L. J. Chen, and Z. L. Wang, Piezoelectric nanogenerator using p-type ZnO nanowire arrays, *Nano Lett.*, 2009, 9(3): 1223